

# Detection of Mercury and Copper Ions Using Surface Plasmon Resonance Optical Sensor

Yap Wing Fen\*, Wan Mahmood Mat Yunus and Nor Azah Yusof

Department of Physics, Faculty of Science, Universiti Putra Malaysia,  
43400 UPM Serdang, Selangor, Malaysia

(Received August 23, 2010; accepted November 25, 2010)

**Key words:** surface plasmon resonance, mercury and copper ions, chitosan, glutaraldehyde

Mercury and copper ions,  $\text{Hg}^{2+}$  and  $\text{Cu}^{2+}$ , can be detected by measuring surface plasmon resonance signals with a thin chitosan layer deposited on a gold film. An amount of 0.55 ml of chitosan cross-linked glutaraldehyde solution was spin coated onto a glass cover slip at 6000 rev./min for 30 s. Changes in the resonance angle ( $\Delta\theta$ ) are directly proportional to the concentration of heavy metal ions in solution (0.5–100 ppm). The sensitivities to  $\text{Hg}^{2+}$  and  $\text{Cu}^{2+}$  are 0.00743 and 0.00654  $\text{ppm}^{-1}$ , respectively. The gold/chitosan interface is highly sensitive to  $\text{Hg}^{2+}$  and  $\text{Cu}^{2+}$  with detection limits as low as 500 ppb.

## 1. Introduction

As a result of industrial development, heavy metal pollution, including mercury and copper, has become a major issue throughout many countries all over the world, owing to their possible toxic effects. As trace elements, heavy metals such as copper are essential to maintain the metabolism of the human body. However, at higher concentrations, they are harmful to human life. Heavy metals are dangerous because they tend to bioaccumulate, that is, the concentration of a chemical in a biological organism increases with time, compared with the concentration in the environment. Exposure to mercury causes loss of myelinated nerve fibers, autonomic dysfunction, and abnormal central nervous system cell division. Mercury poisoning has also recently been linked to neurodevelopmental syndrome and autism. The symptoms of sensory, immune, neurological, motor, and behavioural dysfunctions are associated with autism and mercury poisoning cases. Copper in high doses can cause anemia, liver and kidney damage, and stomach and intestinal irritation.

In Malaysia, heavy metal pollution has grown to a dangerous level. Different techniques for trace metal analysis, including atomic absorption spectroscopy, inductively coupled plasma mass spectroscopy, electrochemical impedance spectroscopy, voltammetry, and polarography, have been widely used but these methods are expensive,

---

\*Corresponding author: e-mail: yapwingfen@gmail.com

sample treatment is complicated and the measurement period is long. Optical sensors including surface plasmon resonance spectroscopy are cost-effective alternatives for this purpose.<sup>(1,2)</sup>

Surface plasmon resonance (SPR) spectroscopy is a surface-sensitive technique<sup>(3)</sup> that has been used to characterize the thickness and refraction index of a dielectric medium at a noble-metal surface.<sup>(4)</sup> In the last decade, surface plasmon resonance sensors have been extensively studied. The surface plasmon resonance technique has emerged as a powerful technique for a variety of chemical and biological sensor applications.<sup>(5)</sup> The first chemical sensing based on SPR technique was reported by Liedberg *et al.* (1983).<sup>(6)</sup> They have demonstrated the use of SPR. SPR is an optical process in which light satisfying a resonance condition excites a charge-density wave propagating along the interface between a metal and a dielectric material using a monochromatic and p-polarized light beam.<sup>(7)</sup> The intensity of the reflected light is reduced at a specific incident angle producing a sharp shadow (called surface plasmon resonance) owing to the resonance energy between the incident beam and surface plasmon wave. SPR is regarded as a simple optical technique for surface and interfacial studies and shows great potential for investigating biomolecules.<sup>(8)</sup> SPR has been widely demonstrated as an effective optical technique for the study of interfaces and thin films.<sup>(9)</sup> A high specificity of the SPR optical sensor to heavy metal ions can be obtained by developing or depositing a thin layer of a suitable material on a gold thin film.<sup>(11-19)</sup>

Chitosan is a copolymer of glucosamine and *N*-acetyl glucosamine linked by  $\beta$ -1,4 glucosidic bonds. Chitosan occurs naturally in some microorganisms, yeast and fungi. Its occurrence is much less widespread than that of chitin. Chitin is a linear chain consisting of *N*-acetyl-D-glucosamine (2-acetamido-2-deoxy- $\beta$ -D-gluconopyranose) joined together by  $\beta$ (1 $\rightarrow$ 4) linkage. It is a nontoxic, biocompatible, and biodegradable natural polymer of high molecular weight (~500,000 kDa). It is the second most common polysaccharide occurring in nature after cellulose. Chitin is found in abundance in the exoskeletons of insects, shells of crustaceans and fungal cell walls. Commercially available chitosan is mostly derived by alkaline *N*-deacetylation from chitin of crustaceans because it is easily obtained from the shells of crabs, shrimps, lobsters, and krill. The structures of chitosan and chitin are shown in Figs. 1(a) and 1(b), respectively.

When chitosan is dissolved in acetic acid, the amino groups ( $-\text{NH}_2$ ) of glucosamine are protonated to  $-\text{NH}_3^+$ . The cationic polyelectrolyte readily forms electrostatic interactions with other anionic groups. In an acidic environment, the majority of polysaccharides are usually neutral or negatively charged. The cationic chitosan molecule interacts with negatively charged surfaces and anionic systems, leading to the modification of the physicochemical characteristics of these systems and ultimately giving rise to its unique functional properties.<sup>(20)</sup> Thus, it has been used in diverse applications such as substrates for drug and enzyme immobilization, separation membranes, and metal adsorbants for the removal of heavy metal.<sup>(21)</sup>

Reports on the combination of chitosan film and the SPR technique are not common. Hence, in this study, we investigate the effect of chitosan film on the SPR signal after the addition of different concentrations of heavy metal ion in solutions:  $\text{Hg}^{2+}$  and  $\text{Cu}^{2+}$ . Thus, we characterized the SPR phenomenon in a simple and reliable optical sensor for the detection of the heavy metals  $\text{Hg}^{2+}$  and  $\text{Cu}^{2+}$  in solution.

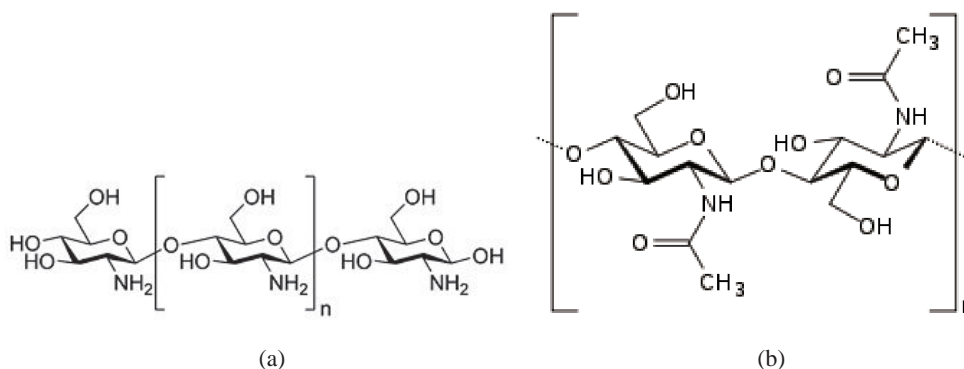


Fig. 1. Structures of (a) chitosan and (b) chitin.

## 2. Materials and Methods

### 2.1 Materials

Chitosan with medium molecular weight and degree of deacetylation 75–85% was purchased from Sigma Aldrich (St. Louis, MO, USA). Acetic acid and glutaraldehyde were also obtained from Aldrich. Standard solutions for mercury, copper, and lead with a concentration of 1,000 ppm were purchased from MERCK (Merck, Darmstadt, Germany).

A prism with refractive index,  $n = 1.77861$  at 632.8 nm, the substrate, and glass cover slips  $24 \times 24 \text{ mm}^2$  of 0.13–0.16 mm thickness were purchased from Menzel-Glaser.

### 2.2 Preparation of heavy metal solutions

Mercury and copper standard solutions with a concentration of 1000 ppm were diluted using the dilution formula,  $M_1V_1 = M_2V_2$ , to produce  $\text{Hg}^{2+}$  and  $\text{Cu}^{2+}$  solutions with concentrations of 0.5, 1, 5, 10, 30, 50, 70, and 100 ppm.

### 2.3 Preparation of chitosan

To prepare a chitosan solution, 0.40 g of chitosan was dissolved in 50 ml of 1% acetic acid. The solution was stirred for 24 h until all the chitosan was dissolved in the acetic acid. Then, 0.05 g of glutaraldehyde was added to the solution to cross-link the chitosan. The resulting solution was stirred for another 1 h.

### 2.4 Preparation of films

The glass cover slips were cleaned using acetone to remove dirt or fingerprint marks on the surfaces of the glass slides. Then, the glass slides were deposited with a 50-nm-thick gold layer using the SC7640 sputter coater.

Spin coating was used to produce a thin layer of chitosan film on top of the gold layer. Approximately 0.55 ml of the solution was placed on the glass cover slip covering

the majority of the surface. The glass cover slip was spun at 6,000 rev./min for 30 s using the spin coating system, P-6708D.

### 2.5 SPR system

Figure 2 shows the experimental setup for SPR measurement. The SPR measurement is carried out by measuring the reflected He-Ne laser beam (632.8 nm, 5 mW) as a function of incident angle. The optical setup consists of a He-Ne laser, an optical stage driven by a stepper motor with a resolution of  $0.001^\circ$  (Newport MM 3000), a light attenuator, a polarizer, and an optical chopper (SR 540). The reflected beam was detected using a sensitive photodiode and then processed using a lock-in amplifier (SR 530).

### 2.6 Sample cell

A cell was constructed to hold and supply the heavy metal solution to the glass cover slip with thin films, as shown in Fig. 3. An open-ended cylindrical brass cavity with an O-ring seal was attached to the glass cover slip that was attached to the prism using index-matching liquid. The heavy metal solution was filled into the hollow formed so that the laser light irradiated the solution. The prism and cell were mounted on a rotating plate to control the angle of the incident light.

## 3. Results and Discussion

First, about 2 ml of deionized water was added into the cell in contact with the gold/chitosan film. From the SPR curve for deionized water, which is shown in Fig. 4, the resonance angle was obtained as  $57.248^\circ$ .

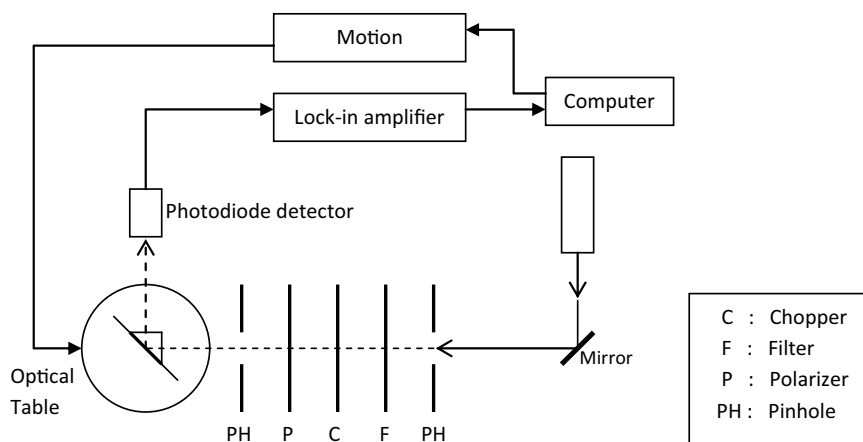


Fig. 2. Experimental setup for angle scan surface plasmon resonance technique.

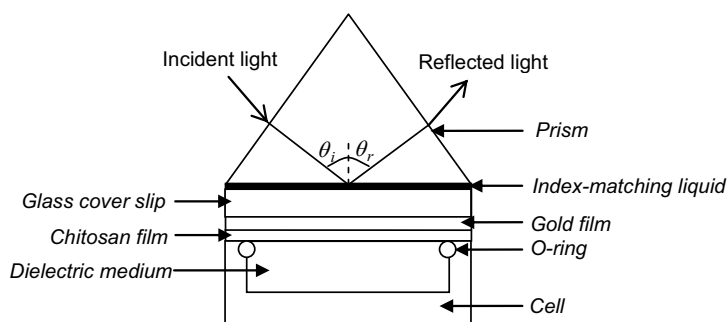


Fig. 3. Structure of the cell for SPR measurement.

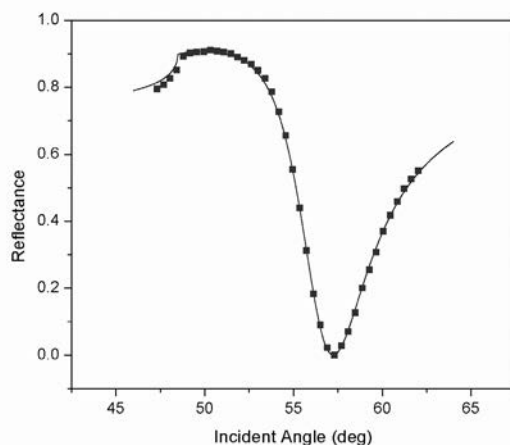


Fig. 4. SPR curve for deionized water in contact with gold/chitosan film.

Different concentrations of  $\text{Hg}^{2+}$  were injected into the cell to be in contact with the gold/chitosan film. After the addition of each sample, the sample was left for 10 min before the SPR curve of the sample was taken. The resonance angles determined from the SPR curves were  $57.236^\circ$ ,  $57.225^\circ$ ,  $57.192^\circ$ ,  $57.153^\circ$ ,  $57.012^\circ$ ,  $56.885^\circ$ ,  $56.746^\circ$ ,  $56.496^\circ$  for  $\text{Hg}^{2+}$  at concentrations of 0.5, 1, 5, 10, 30, 50, 70, and 100 ppm, respectively. We observed that the resonance angle shifted to the left with increasing concentration of  $\text{Hg}^{2+}$  in solution, as shown in Fig. 5.

The change in the SPR resonance angle ( $\Delta\theta$ ) can be determined by taking the differences between the resonance angle of the sample and that of deionized water (as a reference). The relationship between  $\Delta\theta$  and the concentration of  $\text{Hg}^{2+}$  is shown in Fig. 6. A linear relationship with a sensitivity of  $0.00743^\circ \text{ ppm}^{-1}$  and linear regression coefficient of 0.99794 is observed.

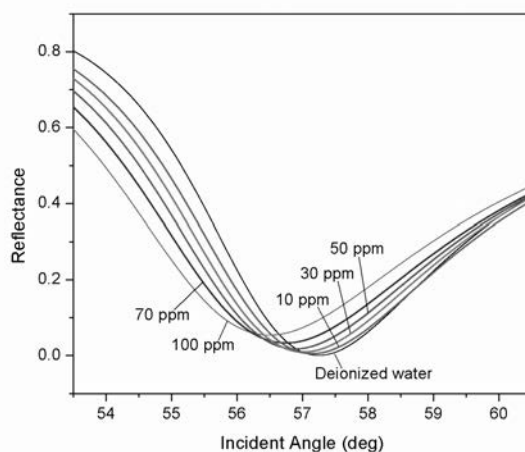


Fig. 5. Optical reflectance as a function of incident angle for gold-chitosan film due to the addition of  $\text{Hg}^{2+}$  with different concentrations, i.e., 10, 30, 50, 70, and 100 ppm.

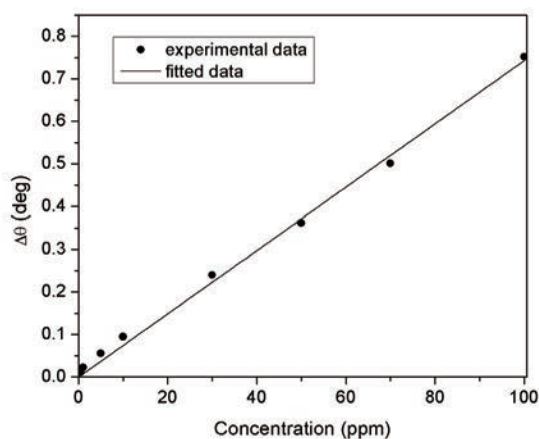


Fig. 6. Change in SPR resonance angle ( $\Delta\theta$ ) versus  $\text{Hg}^{2+}$  concentration.

In this work, we also studied the kinetic behaviour of the heavy metal ion sample by monitoring the self-assembly process on the surface of gold/chitosan in real time. The  $\text{Hg}^{2+}$  sample was injected into the cell and the resulting changes in the resonance angle as a function of time were determined. Figure 7 shows the specific binding of  $\text{Hg}^{2+}$  in real time from solution concentrations as low as 500 ppb (0.5 ppm). From the figure, it was found that the kinetics is complete at approximately 100 s for  $\text{Hg}^{2+}$  at concentrations from 0–5 ppm. For higher concentrations up to 100 ppm, a more complex kinetic

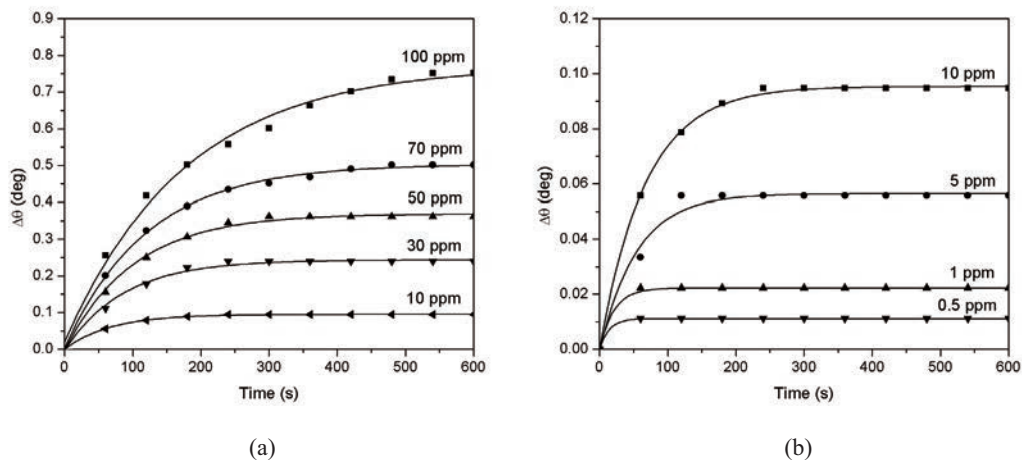


Fig. 7. Change in SPR angle with time upon addition of  $\text{Hg}^{2+}$  (a) from 10 to 100 ppm and (b) from 0.5 to 10 ppm into the cell on gold covered with chitosan film.

profile was observed and it was complete at approximately 500 s. The difference in the kinetic profiles for the high and low concentrations of  $\text{Hg}^{2+}$  is suggested to be due to the interaction and binding of  $\text{Hg}^{2+}$  to the chitosan film. Higher concentrations required more time to interact completely with the film. This shows that the important point in the earlier part of the experiment (left for 10 min before the SPR curve was taken) is to ensure that the reaction between  $\text{Hg}^{2+}$  and the chitosan film is complete for all concentrations.

Similarly, the above processes were applied to another heavy metal ion in solution,  $\text{Cu}^{2+}$ . The resonance angles obtained were  $57.236^\circ$ ,  $57.228^\circ$ ,  $57.200^\circ$ ,  $57.158^\circ$ ,  $57.053^\circ$ ,  $56.924^\circ$ ,  $56.780^\circ$ , and  $56.601^\circ$  for  $\text{Cu}^{2+}$  at concentrations of 0.5, 1, 5, 10, 30, 50, 70, and 100 ppm, respectively.

For each sample, when the concentration of  $\text{Cu}^{2+}$  increased, the resonance angle shifted to a higher value. The change in the resonance angle ( $\Delta\theta$ ) is linearly proportional to the concentration of  $\text{Cu}^{2+}$  as shown in Fig. 8. The slope of the straight line, which reflects the sensitivity of  $\text{Cu}^{2+}$  detection, was estimated to be  $0.00654^\circ \text{ ppm}^{-1}$ . The linear regression coefficient observed was 0.99827.

The kinetic behaviour of  $\text{Cu}^{2+}$  on the gold/chitosan surface was also investigated. The earlier method reported for the  $\text{Hg}^{2+}$  sample was repeated for the  $\text{Cu}^{2+}$  sample. Figure 9 shows the specific binding of  $\text{Cu}^{2+}$  in real time for solution concentrations of 0–100 ppm. Similar to  $\text{Hg}^{2+}$ , the kinetic behaviour of  $\text{Cu}^{2+}$  can be divided into two groups: (1) For concentrations of 0–5 ppm, the kinetic reaction is complete at approximately 100 s. (2) For concentrations of 10 ppm and above, it is complete at

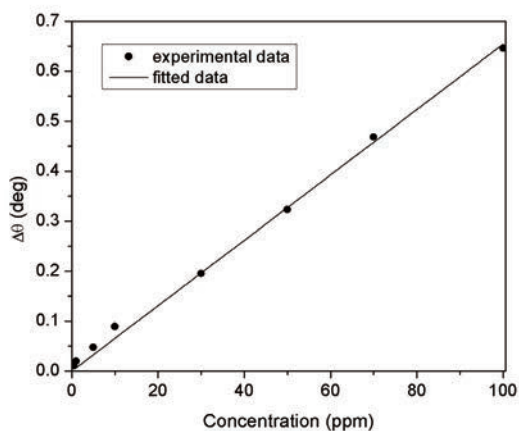


Fig. 8. Change in SPR resonance angle ( $\Delta\theta$ ) versus  $\text{Cu}^{2+}$  concentration.

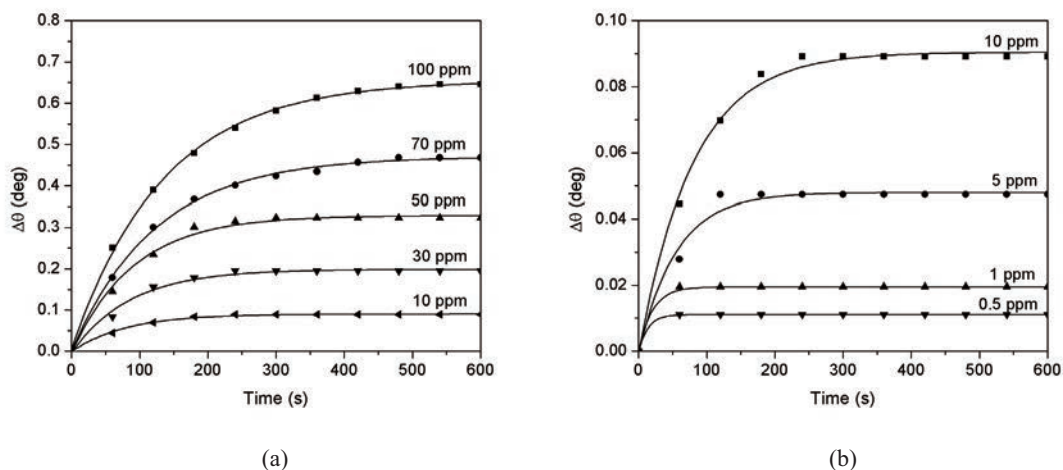


Fig. 9. Change in SPR angle with time upon addition of  $\text{Cu}^{2+}$  (a) from 10 to 100 ppm and (b) from 0.5 to 10 ppm into the cell on gold covered with chitosan film.

about 500 s. We believe that this phenomenon with  $\text{Cu}^{2+}$  is also due to the interaction and conformational rearrangement upon  $\text{Cu}^{2+}$  binding to the chitosan film.

We strongly believe that the chitosan thin film plays an important role in the detection of the heavy metals  $\text{Hg}^{2+}$  and  $\text{Cu}^{2+}$ . This was proved by replacing the gold/chitosan film with only gold film in the experiment. From the results, we observed that there were no changes in the resonance angle for concentrations below 50 ppm for the  $\text{Hg}^{2+}$  and  $\text{Cu}^{2+}$  samples. There was only a slight change for higher concentrations with a sensitivity of 6.038



$\times 10^{-4}$  and  $4.784 \times 10^{-4}$  ppm $^{-1}$  for Hg $^{2+}$  and Cu $^{2+}$ , respectively (Fig. 10). These values are not sufficient for the practical application of the sensor.

Chitosan increases the sensitivity to the detection of Hg $^{2+}$  and Cu $^{2+}$  ions. When the Hg $^{2+}$  or Cu $^{2+}$  ion is attached to the chitosan layer, the Hg $^{2+}$  or Cu $^{2+}$  ion may interact with the chitosan layer owing to the formation of a pair of shared electrons between the positive charge from the Hg $^{2+}$  or Cu $^{2+}$  ion and the negative charge from the amine functional group in chitosan. However, this reaction is not reversible. In this study, we also observed that the sensitivity to Hg $^{2+}$  detection is higher than that for Cu $^{2+}$ . The sensitivities (slope of the graph) are shown in Fig. 11.

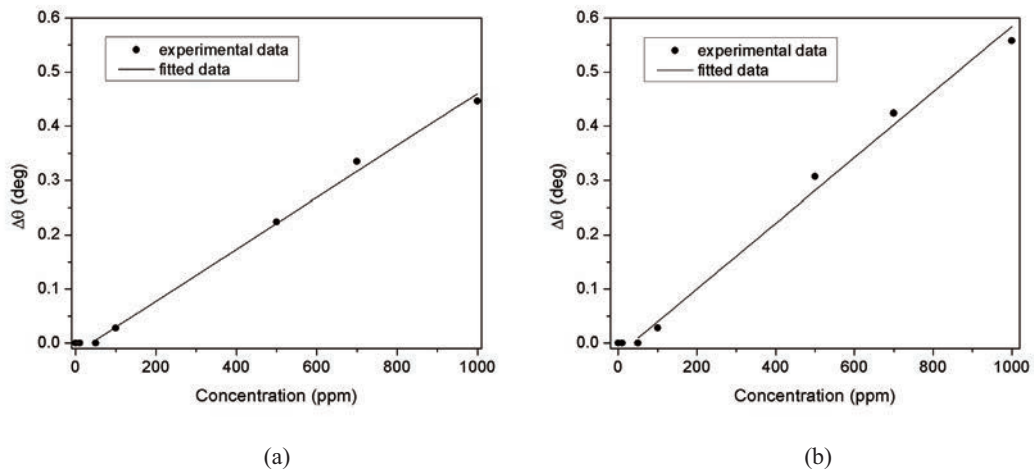


Fig. 10. Change in SPR resonance angle ( $\Delta\theta$ ) versus concentration for (a) Hg $^{2+}$  and (b) Cu $^{2+}$ ; only gold film without chitosan.

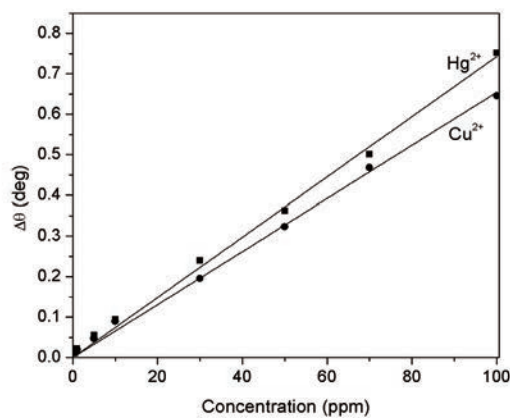


Fig. 11. Change in SPR resonance angle ( $\Delta\theta$ ) versus concentration for Hg $^{2+}$  and Cu $^{2+}$ ; gold/chitosan film.

#### 4. Conclusions

In this work, an SPR optical sensor for the detection of  $\text{Hg}^{2+}$  and  $\text{Cu}^{2+}$  was developed by introducing a chitosan thin film onto a gold layer. The resonance angle shifted to lower values with increasing concentration of  $\text{Hg}^{2+}$  or  $\text{Cu}^{2+}$  in solution. The change in the resonance angle ( $\Delta\theta$ ) is directly proportional to the concentration of those heavy metal ions. The sensitivities to  $\text{Hg}^{2+}$  and  $\text{Cu}^{2+}$  were 0.00743 and 0.00654  $\text{ppm}^{-1}$ , respectively, which shows that the sensor is more sensitive to  $\text{Hg}^{2+}$  than to  $\text{Cu}^{2+}$  in the present work. The kinetic behaviours for both  $\text{Hg}^{2+}$  and  $\text{Cu}^{2+}$  on the gold/chitosan surface were similar. The kinetics is complete at 100 s at concentrations of 0–5 ppm, whereas a more complex kinetic profile was observed for higher concentrations. The above results proved that the SPR optical sensor is a good for detecting heavy metal ions such as  $\text{Hg}^{2+}$  and  $\text{Cu}^{2+}$ .

#### Acknowledgements

The authors would like to thank the Malaysian Government for funding support through SAGA. The laboratory facilities provided by the Department of Physics, Faculty of Science, University Putra Malaysia, are also acknowledged.

#### References

- 1 J. Homola: Surface Plasmon Resonance Based Sensor (Springer, New York, 2006).
- 2 J. Homola, S. S. Yee and G. Gauglitz: Sens. Actuators, B: Chem **54** (1999) 3.
- 3 N. J. Tao, S. Boussaad, W. L. Huang, R. A. Arechabalets and J. D'Agnesse: Rev. Sci. Instrum. **70** (1999) 4656.
- 4 W. Y. W. Yusmawati, H. P. Chuah and W. M. M. Yunus: Am. J. Appl. Sci. **4** (2007) 1.
- 5 H. Q. Zhang, S. Boussaad and N. J. Tao: Rev. Sci. Instrum. **74** (2003) 150.
- 6 B. Liedberg, C. Nylander and I. Lundstrom: Sens. Actuators, B: Chem. **4** (1983) 299.
- 7 K. Kurihara and K. Suzuki: Anal. Chem. **74** (2002) 696.
- 8 C. M. Wu and L. Y. Lin: Sens. Actuators, B: Chem. **110** (2005) 231.
- 9 J. Mendelez, R. Carr, D. Bartholomew, H. Taneja, S. Yee, C. Jung and C. Furlong: Sens. Actuators, B: Chem. **38** (1997) 375.
- 10 S. W. Chah, J. H. Yi and R. N. Zare: Sens. Actuators, B: Chem. **99** (2004) 216.
- 11 C. C. Yu, P. C. Lai and S. Sadeghi: Sens. Actuators, B: Chem. **101** (2004) 236.
- 12 Y. T. Zhang, M. T. Xu, Y. J. Wang, F. Toledo and F. M. Zhou: Sens. Actuators, B: Chem. **123** (2007) 784.
- 13 J. Moon, T. Kang, S. Oh, S. Hong and J. Yi: J. Colloid Interface Sci. **298** (2006) 543.
- 14 S. Hong, T. Kang, J. Moon, S. Oh and J. Yi: Colloids and Surfaces A: Physicochem. Eng. Aspects **292** (2007) 264.
- 15 E. S. Forzani, K. Foley, P. Westerhoff and N. Tao: Sens. Actuators, B: Chem. **123** (2007) 82.
- 16 F. Mirkhalaf and D. J. Schiffrin: J. Electroanal. Chem. **484** (2000) 182.
- 17 A. Sugunan, C. Thanachayanont, J. Dutta and J. G. Hilborn: Sci. Technol. Adv. Mater. **6** (2005) 335.
- 18 S. M. Lee, S. W. Kang and D. U. Kim: Dyes Pigm. **49** (2001) 109.
- 19 C. M. Wu and L. Y. Lin: Biosens. Bioelectron. **20** (2004) 864.
- 20 D. R. Bhumkar and V. B. Pokharkar: AAPS Pharm. Sci. Technol. **7** (2006) 50.
- 21 C. L. Shauer, M. S. Chen, M. Chatterley, K. Eisemann, E. R. Welsh, R. R. Price, P. E. Schoen and F. S. Ligler: Thin Solid Films **434** (2003) 250.